Portland clinker production with carbonatite waste and tire-derived fuel: crystallochemistry of minor and trace elements

(Produção de cimento Portland a partir de resíduos de carbonatito e com combustível derivado de pneus: cristaloquímica de elementos menores e traços)

F. R. D. Andrade[1], M. Pecchio[2], J. M. C. Santos[1], Y. Kihara[1,2]
*[1]Departamento de Mineralogia e Geotectônica, Instituto de Geociências,
Universidade de S. Paulo, S. Paulo, Brasil
[2]Associação Brasileira de Cimento Portland (ABCP), S. Paulo, Brasil
dias@usp.br*

Abstract

This paper presents results on the composition of Portland clinkers produced with non-conventional raw-materials and fuels, focusing on the distribution of selected trace elements. Clinkers produced with three different fuel compositions were sampled in an industrial plant, where all other parameters were kept unchanged. The fuels have chemical fingerprints, which are sulfur for petroleum coke and zinc for TDF (tire-derived fuel). Presence of carbonatite in the raw materials is indicated by high amounts of strontium and phosphorous. Electron microprobe data was used to determine occupation of structural site of both C_3S and C_2S, and the distribution of trace elements among clinker phases. Phosphorous occurs in similar proportions in C_3S and C_2S; while considering its modal abundance, C_3S is its main reservoir in the clinker. Sulfur is preferentially partitioned toward C_2S compared to C_3S. Strontium substitutes for Ca^{2+} mainly in C_2S and in non-silicatic phases, compared to C_3S.
Keywords: tire-derived fuel, carbonatite, clinker, crystallochemistry.

Resumo

Este artigo apresenta dados composicionais de amostras de clínquer Portland produzido com matérias-primas e combustíveis não convencionais, em especial no que diz respeito à distribuição de elementos menores e traços. Foram amostrados clínqueres produzidos com três misturas diferentes de combustíveis, enquanto os demais parâmetros foram mantidos constantes. Os combustíveis apresentam características químicas típicas, como o teor elevado de enxofre no coque de petróleo e o alto teor de zinco no combustível derivado de pneus. O uso de carbonatito como matéria-prima se reflete nos teores elevados de estrôncio e fósforo. Dados de microssonda eletrônica foram usados para determinar a ocupação de sítios estruturais de C_3S e C_2S, e para modelar a distribuição de elementos traços entre as fases do clínquer. O fósforo ocorre em proporções similares em C_3S e C_2S; se considerarmos sua abundância modal, o C_3S é o principal reservatório de fósforo no clínquer. O enxofre é preferencialmente concentrado em C_2S em comparação com C_3S. O estrôncio substitui Ca^{2+} principalmente em C_2S e em fases não-silicáticas, em comparação com C_3S.
Palavras-chave: *combustível derivado de pneus, carbonatito, clínquer, cristaloquímica.*

INTRODUCTION

The chemical composition of Portland clinker is determined by the composition of its raw materials and fuels. The proportion of major components (SiO_2, CaO, Al_2O_3, Fe_2O_3, MgO) of the raw mix is well constrained, in order to form the main crystalline phases of the clinker (C_3S, C_2S, C_3A, C_4AF) in adequate proportions. The chemical composition of the system is affected by cofiring of residues, as well as non-traditional raw-materials and fuels. Intake of trace elements as solid solutions in the structure of crystalline phases is controlled by the ionic radius and charge of the elements, and solid solution may affect the lattice parameters and the stability of polymorphs. Chemical

variability is particularly noticeable in trace elements concentration, because their small absolute abundances, typically in ppm range, make possible much larger relative variation in comparison to the major components.

In the present study, clinker samples of industrial clinker from a plant in southern Brazil have been investigated because of their unusual content in trace elements, due to both raw materials and fuel composition. The carbonatic raw-material for this cement plant is the waste from a neighboring carbonatite-related phosphate mine and, therefore, is particularly rich in phosphate. Carbonatites are rare magmatic rocks, formed by solidification of carbonate magmas that rise from the Earth´s mantle into the crust [1]. The magmatic origin of carbonatites was recognized in the

beginning of the XX century, based on their field relations, mineralogical and chemical composition, particularly their high contents of trace elements that are nearly absent in limestones and marbles, such as strontium and rare earth elements (lanthanides). Other source of trace elements in the plant is the fuel, which comprises coal, petroleum coke (pet coke) and tire derived fuel (TDF), the latter is used in the plant since 2003. Pet coke is the leading fuel in cement plants in Brazil, corresponding to 71% of the energy consumption of the cement industry in the country [2].

Combination of the chemical composition of whole-clinker samples, modal composition (point counting and XRD-Rietveld) and the chemical composition of Ca-silicates allow some considerations on the partition of selected trace elements (P, S, Sr, Mg) among the crystalline phases of the clinker. Clinker sampling was done in three distinct compositions of the fuel, as described in the next session. The present study aims to assess the impact of tire-derived fuel on clinker composition and to trace back the paths followed by single chemical elements.

MATERIALS AND METHODS

The studied clinker samples are produced in a plant in southeastern Brazil. The carbonatitic raw-material used for cement production comes from the mine tailings of a neighboring apatite open-pit mine (apatite general formula, $Ca_3(PO_4)_3(OH, F, Cl)$). Mineralogical composition of the mine tailings is mainly calcite and dolomite, with minor amounts of apatite, magnetite and phlogopite. The phosphate deposit is situated in the Jacupiranga carbonatite-pyroxenite complex [3].

The fuel used in the cement plant is a mixture of coal, petroleum coke and TDF, which approximate proportion in terms of heat content is 65, 15 and 20%, respectively. Most of the iron necessary for clinker production is provided by the metallic structure of the whole tires. The organic fraction of the tires is destroyed by burning, while their metallic structure and inorganic fillers are added to the clinker composition.

TDF combines scrap tires, which are continuously fed to the kiln, and whole tires, which are fed to the kiln in regular intervals of ca. 30 s each. For this particular study, the current fuel composition was changed, in order to assess the effect of the fuel on the chemical and mineralogical composition of the clinker. Fuel compositions during clinker sampling were: (A) pet coke + coal + scrap waste tires + whole waste tires, which is the current fuel used in the plant; (B) pet coke + coal + scrap waste tires; (C) pet coke + coal. Capital letters A, B and C are used throughout this paper to indicate fuel composition. For each fuel composition, five samples of clinker (5 kg each) were collected in the lifter to the silo, one sample per hour; each clinker sample is composed by the five sub-samples, that were checked for their compositional homogeneity and mechanically mixed. Clinker sampling started two hours after changing the fuel composition, for the system to reach equilibrium and avoid major oscillations in composition.

Electron microprobe (EM) analyses of calcium silicates were carried out in a JEOL 8600 equipment, at the Geoanalítica-USP Facility (University of S. Paulo, Brazil), with a wavelength dispersive spectrum (WDS) detector, with 20 nA current, 15 kV and a 5 μm-diameter of the electron beam. Mineral composition in wt.% of oxides was converted in cationic proportion based on 20 oxygen atoms per formula, which is the least common multiple of oxygen atoms in the ideal formulae of both Ca-silicates, i.e. the structural formulae of Ca_3SiO_5 (C_3S or alite) and Ca_2SiO_4 (C_2S or belite) are presented as $Ca_{12}Si_4O_{20}$ and $Ca_{10}Si_5O_{20}$, respectively. Thirty EM analyses were made for both C_3S and C_2S in each clinker sample. EM analysis of interstitial phases (C_4AF, C_3A, MgO) did not yield good results, because of the relatively small size (<10 μm) of individual crystals and their irregular surface in polished samples. Based on their ion radius [4], cations were distributed among crystallographic sites. Smaller cations, including S^{6+} (0.12 Å), P^{5+} (0.17 Å), Al^{3+} (0.39 Å), Ti^{4+} (0.42 Å) and Fe^{3+} (0.49 Å), were allocated in the tetrahedral site, ideally occupied by Si^{4+} (0.26 Å). Larger cations, including Sr^{2+} (1.18 Å), Mn^{2+} (0.83 Å), Zn^{2+} (0.74 Å) and Mg^{2+} (0.72 Å), were allocated in the octahedral site, ideally occupied by Ca^{2+} (1.00 Å). The most reliable data were selected with the criteria of oxide summation close to 100 wt.%, adequate proportion of cations in tetrahedral and octahedral sites and charge balance.

Clinker chemical composition of major elements was determined by X-ray fluorescence (XRF) in a RIX-2000 Rigaku spectrometer, and trace elements were analyzed by atomic absorption in a Unicam 939 equipment. X-ray powder diffraction (XRD) was carried out in a Bragg-Brentano Rigaku RINT2000 equipment with Cu kα radiation, 40 kV, 40 mA, step scanning mode (0.01 º/step, 10 s/step) from 18 to 90º 2θ. Samples were back loaded in flat sample holders. Instrumental contribution to peak broadening was assessed with a cerium oxide (CeO_2) standard. Rietveld refinements were made with High Score Plus 3.0 (Panalytical). Rietveld refinement strategy comprised background fitting, scale factor for individual phases, sample displacement, cell parameters for all phases and Gaussian broadening. Peak profile was simulated using the pseudo-Voigt function. Effects of preferential orientation were corrected with a March-Dollase algorithm for C_3S ($\overline{1}01$) and MgO (001). Occupation factor of Al and Fe in C_4AF was also refined. Isotropic thermal parameter (B) was refined for the more abundant phases (C_3S, C_2S, C_4AF). Crystallographic information files (CIFs) of the phases were tested and the following were chosen: monoclinic C_3S [5]; monoclinic C_2S [6]; isometric C_3A [7]; C_4AF [8]; MgO [9]; CaO [10]; $Ca(OH)_2$ [11]. Other polymorphs were searched for and not detected, including triclinic and rhombohedral C_3S, orthorhombic C_2S and orthorhombic C_3A.

Modal analysis by point counting under the optical microscope was made in polished sections, with 3000 points/sample, followed by density correction for each phase.

RESULTS AND DISCUSSION

Chemical composition of the clinkers produced with the three types of fuel is similar (Table I), except for differences in the contents of transition metals. Zn is the most reliable chemical tracer of the presence of TDF in the fuel. Zinc content is more than seven times higher in clinkers produced with TDF ($X^{Zn}_{Clinker\,B}$= 571 ppm; $X^{Zn}_{Clinker\,A}$ = 517 ppm), compared to clinker produced in the same plant, with TDF-free fuel ($X^{Zn}_{Clinker\,C}$ = 74.9 ppm). Clinker C (TDF-free) is also slightly lower in Fe_2O_3 (3.68 wt.%), compared to A (4.14 wt.%) and B (4.11 wt.%), which causes a slightly higher alumina module in the former (AM = Al_2O_3/Fe_2O_3); other metals (Cr, Co, Cu, Sn) are also lower in clinker C (TDF-free) compared to clinkers A and B. Differences in metal concentration in the clinkers are related to the metallic structure of the tires used in TDF. Concentration of SO_3 in the clinker samples range between 1.2 and 1.9 wt.%; the main source of sulfur in this system is the petroleum coke, with SO_3 (equivalent) contents ranging between 1 and 6 wt.%. Strontium (SrO = 0.8 wt.%) and phosphorous (P_2O_5 = 0.8 to 0.9 wt.%) are relatively high in the analyzed clinker samples, due to the raw-material of magmatic origin (carbonatite). Dolomite in the raw material also lead to relatively MgO-rich high contents (MgO = 6.7 wt.%).

The mineralogical composition of the clinker samples is presented in Table II. Quantitative phase analysis made by XRD-Rietveld and by optical point counting are in good agreement. Clinker A has the highest (C_3S/C_2S) ratio, indicating that the kiln set up had a better performance while operating in its normal, TDF-bearing fuel composition (A), compared to the two other fuel compositions (B, C) used during in this study. C_3S contents range from 43 to 55 wt. %, which are relatively low for an ordinary clinker and are probably related to the presence of phosphorus and strontium in significant amounts in the raw meal. Average concentration of P_2O_5 in ordinary Portland clinker are around 0.2 wt.% [12]. Higher amounts of P_2O_5 inhibits C_3S formation, increasing C_2S and free lime [13-15]. According to [12], strontium is preferentially hosted by C_2S and also inhibits C_3S formation. In the present study, although C_3S is relatively low (45-55 wt.%) compared to C_2S (30-35 wt.%), free lime is also low (< 1.5 wt.%). It indicates that in a complex chemical environment, where not only P_2O_5 is high, but also SrO, MgO, ZnO, as well as S, effects counteract and ideal relations are not maintained.

The Rietveld diagram of clinker A is shown in Fig. 1. Statistical agreement indicators in Rietveld refinements are similar in the three clinker samples (Table II), with Rwp ranging from 12.4 to 14.6 and χ^2 from 4.8 and 5.6; for details on the agreement indexes, see [16, 17]. The difference between CaO determined by point counting and by XRD-Rietveld is smaller if $Ca(OH)_2$ is considered, formed by hydration of CaO during sample handling and XRD data acquisition (Table II).

Regarding the chemical composition of the Ca-silicates, determined with the electron microprobe (Table III), both

Table I - Chemical composition of studied clinkers. A, B and C indicate fuel composition (see text for details). LSF = lime saturation factor; SM = silica module; AM = alumina module.
[Tabela I - Composição química dos clínqueres estudados. A, B e C indicam a composição do combustível (ver texto para detalhes). LSF = fator de saturação em cal; SM = módulo de sílica; AM = módulo de alumina.]

	clinker A	clinker B	clinker C
CaO (wt.%)	60.7	60.0	60.5
SiO_2	19.8	19.5	19.7
Al_2O_3	3.40	3.61	3.77
Fe_2O_3	4.14	4.11	3.68
SO_3	1.24	1.93	1.77
MgO	6.74	6.73	6.71
K_2O	0.24	0.28	0.24
Na_2O	0.03	0.03	0.01
TiO_2	0.38	0.38	0.40
SrO	0.79	0.77	0.79
P_2O_5	0.82	0.88	0.88
MnO	0.20	0.20	0.19
LOI	0.80	0.80	0.61
Sum	99.3	99.2	99.3
Be (ppm)	1.09	0.75	1.10
Cr	90.3	94.5	88.8
Co	32.2	33.2	27.5
Ni	67.4	61.3	66.2
Cu	64.1	57.8	41.4
Zn	517	571	74.9
Cd	0.21	0.33	0.27
Sn	5.49	9.51	2.39
Te	5.22	6.47	4.40
Pb	4.29	7.38	6.63
As	1.41	1.69	1.41
LSF	97.7	97.3	97.5
SM	2.62	2.53	2.64
AM	0.82	0.88	1.02

C_3S and C_2S display slight differences for the three fuel compositions (A, B, C), but there is no straightforward trend for all elements.

The average chemical composition of the calcium silicates determined by electron microprobe (Table III) reveals that C_3S has higher contents of MgO and CaO than C_2S, while all other major elements are more concentrated in C_2S. The minor elements Zn and Mn do not show a marked partition between both silicates. C_3S in clinker C (without TDF) has lower Zn, a trend not observed in C_2S. [18, 19] have shown that Zn does not influence phase formation in clinker, particularly in free lime abundance, while in normal concentration and up to 20 times higher concentrations.

Table II - Modal analysis of clinker samples by Rietveld X-ray diffraction (XRD-R) and by point counting. A, B and C indicate fuel composition (see text for details). Agreement indexes of Rietveld refinements: weighted-profile residue, R_{wp}; goodness-of-fit, c^2.

[Tabela II - Dados de análise modal de amostras de clínquer obtidos por difração de raios X - método de Rietveld (XRD-R) e por contagem de pontos. A, B e C indicam a composição do combustível (ver texto para detalhes). Parâmetros estatísticos de convergência do método de Rietveld: resíduo ponderado, R_{wp}; qualidade de ajuste, c^2.]

	clinker A		clinker B		clinker C	
	XRD-R	*point counting*	*XRD-R*	*point counting*	*XRD-R*	*point counting*
C_3S	52.4	55.3	43.3	45.5	48.3	48.4
C_2S	29.7	26	34.4	35.7	31.9	30.7
C_4AF	11.9	11.9	12.4	12.3	11	12.4
C_3A	0.5	1.6	2.5	2.1	3.1	3.3
MgO	4.9	4.2	6.4	3.7	5.2	4
CaO	0.3	1	0.2	0.7	0.2	1.3
$Ca(OH)_2$	0.4	0	0.8	0	0.3	0
Sum	100	100	100	100	100	100
(C_3S/C_2S)	1.77	2.13	1.26	1.27	1.27	1.51
R_{wp}	*12.8*	--	*12.4*	--	*14.6*	--
c^2	*5.2*	--	*4.8*	--	*5.6*	--
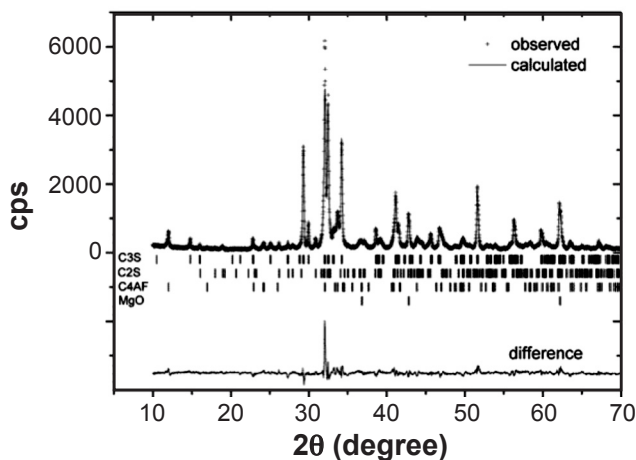
Figure 1: Rietveld plot of the clinker sample A, the current clinker produced in the plant with a fuel mix composed by pet coke, coal, scrap waste tires and whole waste tires. Peak positions of the main crystalline phases are indicated.

[Figura 1: Diagrama de Rietveld plot da amostra de clínquer A, que é o material regularmente produzido na fábrica, com mistura de combustíveis incluindo coque de petróleo, carvão, pneus picados e pneus inteiros. A posição dos picos das principais fases cristalinas é indicada.]

Conversion of absolute concentration (wt.%) in cationic proportion eliminates the differences in atomic mass among the elements and allows a more accurate perception of site occupancy, constrained mainly by the ionic radius and charge (Table III). Cationic proportion, normalized for a given number of oxygen atoms, represents the relative stoichiometric occupancy of the structural sites of crystalline materials. Therefore, the structural formulae of both silicates in the three fuel composition may be written

as in Table IV, with the same data presented in Table III. The calculated formulae differ from those determined by [20]: $C_3S = 3(Ca_{0.98}\ Mg_{0.01}\ Al_{0.067}\ Fe_{0.0033})\ [(Si_{0.97}\ Al_{0.03})\ O_5$; and $C_2S = 2(Ca_{0.975}\ K_{0.01}\ Na_{0.05}\ Mg_{0.01})\ (Si_{0.9}\ Al_{0.06}\ S_{0.01}\ Fe_{0.02})\ O_{3.9}$, indicating that composition of Ca-silicates in clinker depends on the chemical environment in the kiln, which is a consequence of raw-mix and fuel compositions. Therefore, actual compositions proposed by [20] may not be taken as an *a priori* real composition of Ca-silicates of Portland clinker.

A simpfied structure was assumed for both silicates, with a smaller, tetrahedral site occupied by Si, and a larger site, octahedral, occupied by Ca. Substitution of foreign ions for Ca in the octahedral site ("oct"), and for Si in the tetrahedral site ("tetr") may be observed. In both silicates, the tetrahedral site is by far more subjected to substitutions than the octahedral site. The proportion of cation substitution in tetrahedral and octahedral sites in descending order is C_2S_{tetr} (13 to 27% substitution) > C_3S_{tetr} (8.5 to 15% substitution) > C_3S_{oct} (1.2 to 6.2% substitution) > C_2S_{oct} (1 to 4.5% substitution). Cationic substitutions in C_3S and C_2S are plotted in Figs. 2 and 3, respectively.

The extent of substitution in each site is presented in box charts for C_3S and C_2S in Figs. 4 and 5, respectively. Regardless fuel composition, C_3S shows a regular trend, in which the tetrahedral site (C_3S_{tetr}) shows the same order of cation substitution for Si (Al > P > Fe > S > Ti) (Fig. 4a, b, c), and also the same in the octahedral site (C_3S_{oct}) for Ca (Mg >> Sr ≥ Mn ≈ Sr) (Fig. 4d, e, f). C_2S has a slightly different occupancy of the tetrahedral site (C_2S_{tetr}) depending on fuel composition: Al is the major substitute for Si in all cases, and Ti the minor, with P and S alternate positions with different fuel compositions (Fig. 5a, b,

Table III - Average chemical composition (*n* = number of samples) and cationic proportion to 20 oxygen atoms per unit formula of C_3S and C_2S. A, B and C indicate fuel composition (see text for details). Ionic radii considered for cationic distribution among tetrahedral and octahedral sites according to [4].

[Tabela III - Composição química média (n = número de amostras) e proporção catiônica na base de 20 átomos de oxigênio por fórmula unitária de C_3S e C_2S. A, B e C indicam a composição do combustível (ver texto para detalhes). Os raios iônicos considerados na distribuição dos cátions entre sítios tetraédricos e octaédricos segundo [4].]

	C_3S			C_2S		
	A	B	C	A	B	C
n	*18*	*20*	*19*	*11*	*10*	*17*
wt.%						
CaO	71.0	71.7	71.2	63.1	62.2	62.8
SiO_2	23.5	23.0	22.7	27.4	26.2	28.3
MgO	1.53	1.12	1.49	0.25	0.61	0.22
Al_2O_3	1.17	1.45	1.72	2.12	2.50	1.97
Fe_2O_3	0.71	0.74	0.66	1.70	2.13	1.17
SO_3	0.30	0.26	0.34	2.75	2.22	1.89
ZnO	0.04	0.04	0.02	0.02	0.02	0.02
SrO	0.49	0.48	0.55	1.07	1.18	1.09
P_2O_5	0.87	0.94	0.90	1.38	1.60	1.29
TiO_2	0.24	0.22	0.23	0.36	0.56	0.32
MnO	0.08	0.06	0.09	0.03	0.11	0.04
K_2O	0.01	0.01	0.01	0.10	0.16	0.09
total	100.0	100.1	99.9	100.3	99.4	99.2
cationic proportion to 20 atoms of oxygen						
tetrahedral site						
Si	3.57	3.51	3.46	3.95	3.82	4.13
Al	0.21	0.26	0.31	0.36	0.44	0.34
P	0.11	0.12	0.12	0.17	0.20	0.16
Fe	0.08	0.08	0.08	0.18	0.25	0.13
S	0.03	0.03	0.04	0.30	0.24	0.21
Ti	0.03	0.02	0.03	0.04	0.06	0.04
sum tetrahedral	4.04	4.03	4.02	5.0	5.00	5.00
*total charge**	*16.1*	*15.9*	*15.9*	*19.7*	*19.7*	*19.8*
octahedral site						
Ca	11.6	11.7	11.6	9.73	9.73	9.79
Mg	0.35	0.26	0.34	0.05	0.13	0.05
Zn	0.00	0.00	0.00	0.00	0.00	0.00
Mn	0.01	0.01	0.01	0.00	0.02	0.00
Sr	0.04	0.04	0.05	0.09	0.10	0.09
K	0.00	0.00	0.00	0.02	0.03	0.02
sum octahedral	12.0	12.0	12.0	9.90	10.0	9.96
*total charge**	*24.0*	*24.1*	*24.1*	*19.8*	*20.0*	*19.9*

* total charge refers to the sum of cations charge weighted by their cationic proportion in each site

c); Fe is lower in C_3S and C_2S of clinker C (TDF-free), compared to the Ca-silicates of clinkers produced with TDF. The C_2S_{oct} has an occupation with the same trend Sr ≥ Mg >> Mn ≈ Zn in clinker samples produced with three different fuel compositions (Fig. 5d, e, f). Sr^{2+} and Ca^{2+} have the same charge and close ionic radii (1.00 Å and 1.18 Å, respectively), which are the main factors that control the extent of solid solutions. In spite of their similarity, Sr^{2+} is

the most prominent substitution in C_2S, but only a minor substitution in C_3S, indicating that C_3S is more restrictive or less flexible to accommodate cations larger than Ca^{2+} in its octahedral site.

Inside the kiln, matter is distributed between a solid fraction, mainly composed of Ca-silicates formed by solid state reactions, a minor fraction of melt, which form the interstitial phases after cooling and crystallization, and a

Table IV - Average structural formulae for C_3S and C_2S, with cationic proportion on the base of 20 atoms of oxygen (n = number of data).

[Tabela IV - Fórmulas estruturais médias de C_3S e C_2S, com proporção catiônica na base de 20 átomos de oxigênio por fórmula unitária (n = número de amostras).]

phase	fuel	Formula	n
C_3S	A	$(Ca_{11.57} \, Mg_{0.35} \, Sr_{0.04} \, Mn_{0.01}) \, (Si_{3.57} \, Al_{0.21} \, P_{0.11} \, Fe_{0.08} \, S_{0.03} \, Ti_{0.03}) \, O_{20}$	18
	B	$(Ca_{11.72} \, Mg_{0.26} \, Sr_{0.04} \, Mn_{0.01}) \, (Si_{3.51} \, Al_{0.26} \, P_{0.12} \, Fe_{0.08} \, S_{0.03} \, Ti_{0.02}) \, O_{20}$	20
	C	$(Ca_{11.64} \, Mg_{0.34} \, Sr_{0.05} \, Mn_{0.01}) \, (Si_{3.46} \, Al_{0.31} \, P_{0.12} \, Fe_{0.08} \, S_{0.04} \, Ti_{0.03}) \, O_{20}$	19
C_2S	A	$(Ca_{9.73} \, Sr_{0.09} \, Mg_{0.05} \, K_{0.02}) \, (Si_{3.95} \, Al_{0.36} \, S_{0.30} \, Fe_{0.18} \, P_{0.17} \, Ti_{0.04}) \, O_{20}$	11
	B	$(Ca_{9.73} \, Mg_{0.13} \, Sr_{0.10} \, Mn_{0.01} \, K_{0.03}) \, (Si_{3.82} \, Al_{0.44} \, Fe_{0.25} \, S_{0.24} \, P_{0.20} \, Ti_{0.06}) \, O_{20}$	10
	C	$(Ca_{9.79} \, Sr_{0.09} \, Mg_{0.05} \, K_{0.02}) \, (Si_{4.13} \, Al_{0.34} \, S_{0.21} \, P_{0.16} \, Fe_{0.13} \, Ti_{0.04}) \, O_{20}$	17
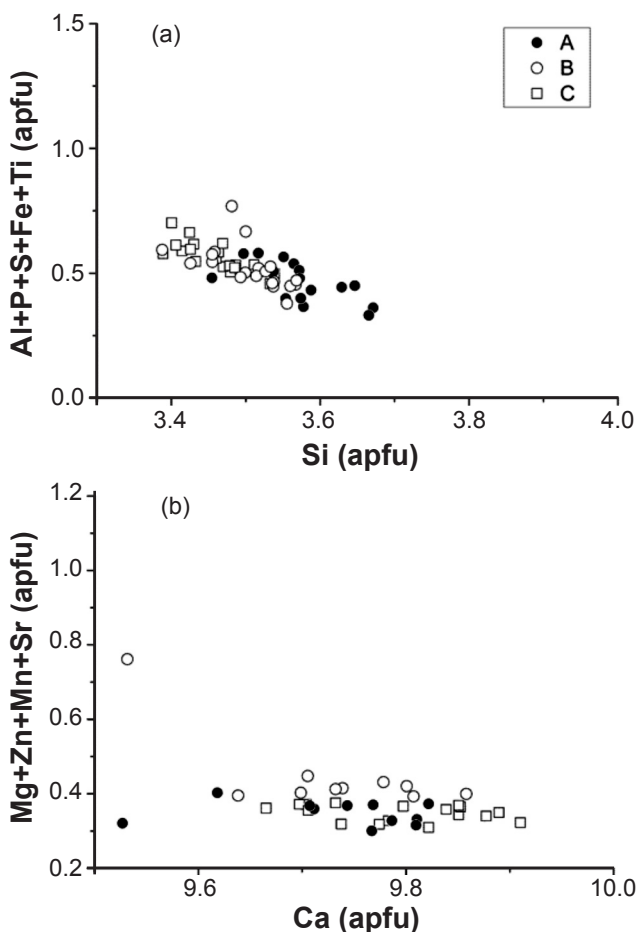
Figure 2: Cationic substitution in (a) tetrahedral and (b) octahedral sites of C3S (apfu - atoms per formula unit). A, B and C indicate fuel composition (see text for details).

[Figura 2: Substituição catiônica nos sítios (a) tetraédrico e (b) octaédrico de C_3S (apfu - átomos por fórmula unitária). A, B e C indicam a composição do combustível (ver texto para detalhes).]
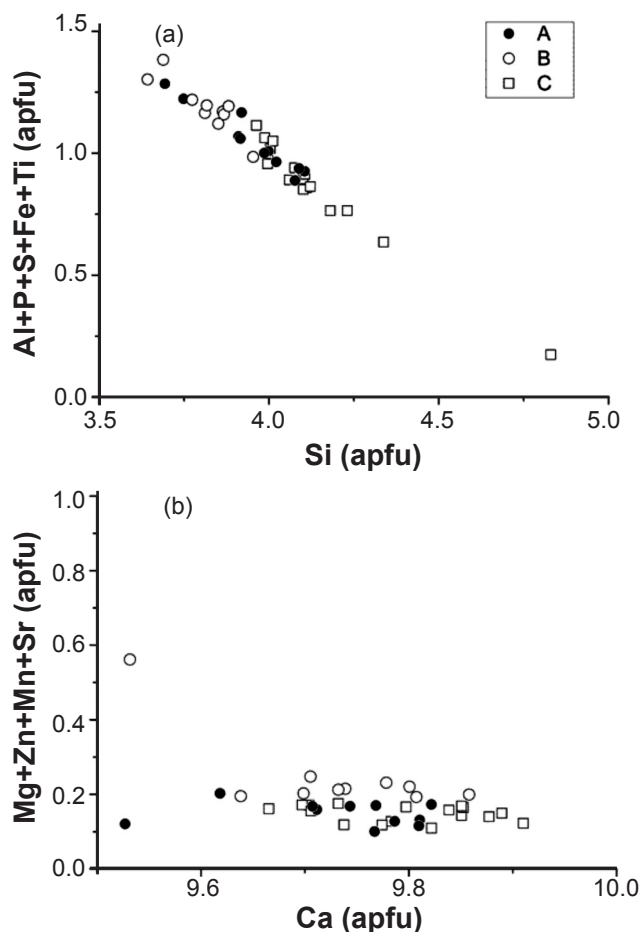
Figure 3: Cation substitution in (a) tetrahedral and (b) octahedral sites of C2S (apfu - atoms per formula unit). A, B and C indicate fuel composition (see text for details).

[Figura 3: Substituição catiônica nos sítios (a) tetraédrico e (b) octaédrico de C_2S (apfu - átomos por fórmula unitária). A, B e C indicam a composição do combustível (ver texto para detalhes).]

vapor phase, that concentrates the volatile compounds and is lost or forms cycles inside the kiln, which may be written as

$$X^S_{clinker} = X^S_{solid\,phase} + X^S_{liquid\,phase} - X^S_{gas\,phase} \qquad (1)$$

In which X expresses the concentration of a given element (for instance S, for sulfur), in a given phase.

In the present paper, we are concerned with the distribution of trace elements among the crystalline phases
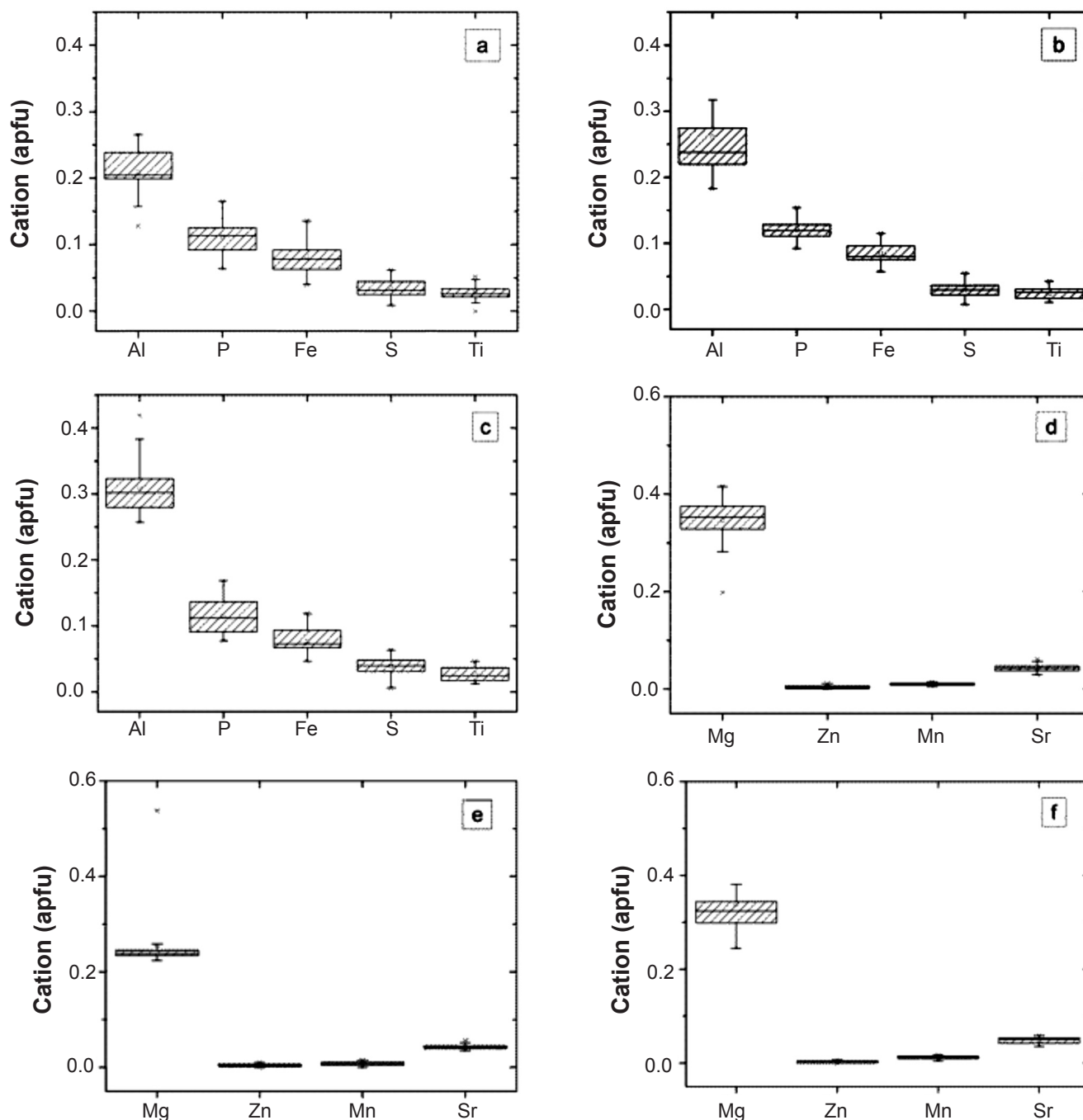
Figure 4: Box chart of the atomic proportion of cations that enter the structural sites of C3S. Tetrahedral site: a = clinker A; b = clinker B; c = clinker C. Octahedral site: d = clinker A; e = clinker B; f = clinker C (apfu – atoms per formula unit). The box displays minimum value, average value, 25%, 50% and 75% of all data, and maximum value. A, B and C indicate fuel composition (see text for details).

[Figura 4: Diagrama tipo 'box chart' das proporções catiônicas presentes nos sítios estruturais de C_3S. Sítio tetraédrico: a = clínquer A; b = clínquer B; c = clínquer C. Sítio octaédrico: d = clínquer A; e = clínquer B; f = clínquer C (apfu – átomos por fórmula unitária). O diagrama apresenta os valores mínimo, médio e máximo, além de 25%, 50% e 75% de todos os dados. A, B e C indicam a composição do combustível (ver texto para detalhes).]

of the clinker; the behavior of the elements toward the gas phase is beyond our present objectives.

As the mass of the clinker is the sum of the masses of all phases, the concentration of a given element in the clinker, for example sulfur (S), is given by the concentration of sulfur in C_3S multiplied by the mass fraction of C_3S, plus the concentration of sulfur in C_2S multiplied by the mass fraction of C_2S, and so on, which can be expressed as

$$X_{clinker}^{S} = f_{C3S}X_{C3S}^{S} + f_{C2S}X_{C2S}^{S} + f_{C4AF}X_{C4AF}^{S} + f_{C3A}X_{C3A}^{S} + f_{CaO}X_{CaO}^{S} \quad (2)$$

where X is the concentration (wt.%) of the element indicated
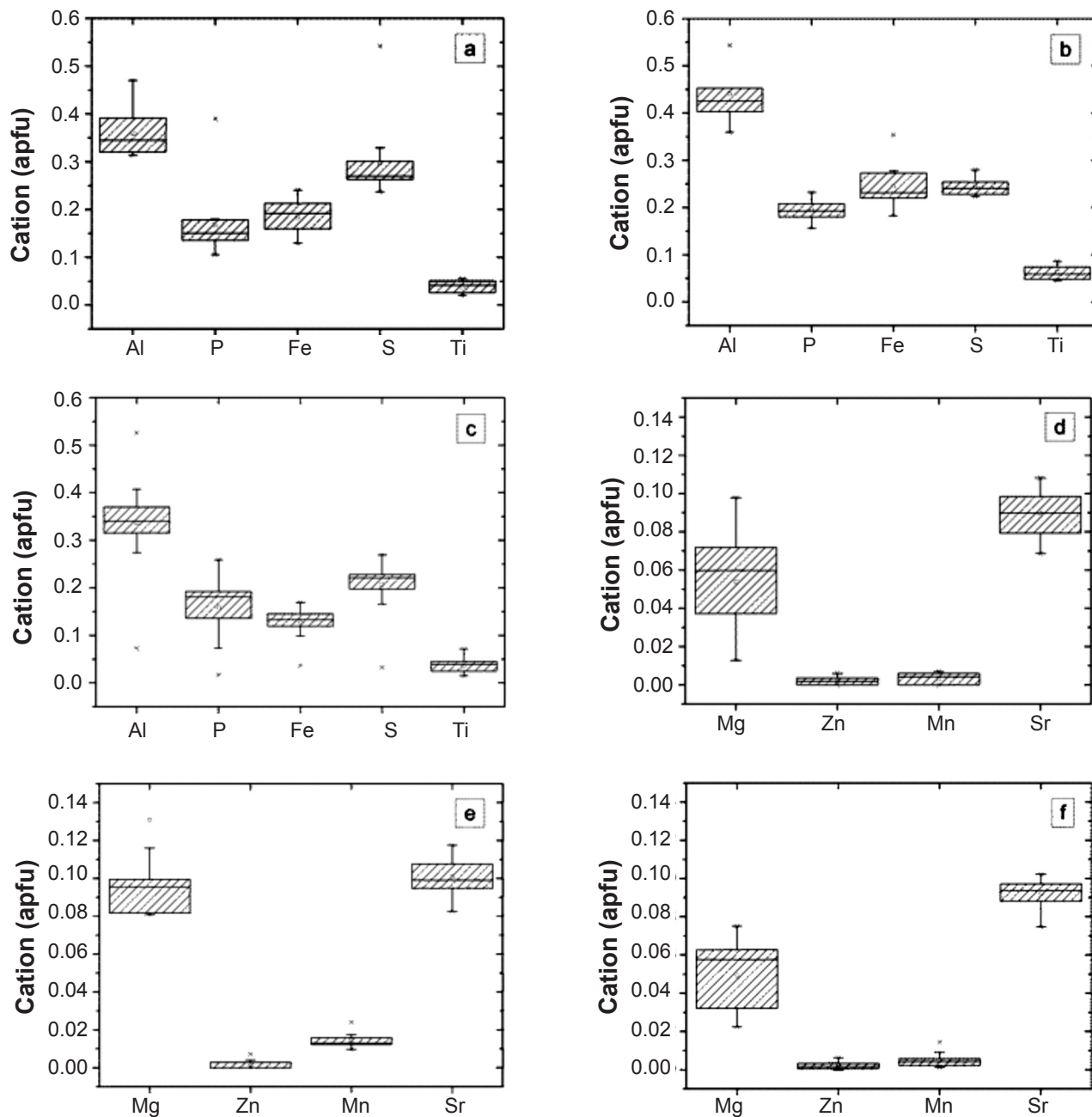
Figure 5: Box chart of the atomic proportion of cations that enter the structural sites of C_2S. Tetrahedral site: a = clinker A; b = clinker B; c = clinker C. Octahedral site: d = clinker A; e = clinker B; f = clinker C (apfu - atoms per formula unit). The box displays minimum value, average value, 25%, 50% and 75% of all data, and maximum value. A, B and C indicate fuel composition (see text for details).
[Figura 5: Diagrama tipo 'box chart' das proporções catiônicas presentes nos sítios estruturais de de C_2S. Sítio tetraédrico: a = clínquer A; b = clínquer B; c = clínquer C. Sítio octaédrico: d = clínquer A; e = clínquer B; f = clínquer C (apfu - átomos por fórmula unitária). O diagrama apresenta os valores mínimo, médio e máximo, além de 25%, 50% e 75% de todos os dados. A, B e C indicam a composição do combustível (ver texto para detalhes).]

in superscript (for instance S, for sulfur) in the phase indicated in subscript (C_3S etc.), while f is the mass fraction (modal abundance) of each respective phase, considering that the fraction mass of the clinker equals the unity and is the summation of the mass fractions of all phases.

Since we determined the chemical composition of the Ca-silicates and their modal proportion in the clinker, which comprise around 80 wt.% of the studied clinkers, we can calculate the individual role of each phase as a reservoir of

a given element. The interstitial phases were not analyzed under the electron microprobe, but their average composition can be assumed to be the overall composition of the clinker minus the composition of the Ca-silicates multiplied by their modal abundance. Therefore, equation (2) can be rewritten as

$$X_{clinker}^{S} = f_{C3S}X_{C3S}^{S} + f_{C2S}X_{C2S}^{S} + f_{other\ phases}X_{other\ phases}^{S} \quad (3)$$

As the mass fraction of other phases is $(1 - f_{C3S} - f_{C2S})$,

the concentration of a given element in the clinker can be expressed by

$$X^s_{clinker} = f_{C3S}X^s_{C3S} + f_{C2S}X^s_{C2S} + (1\text{-}f_{C3S}\text{-}f_{C2S})\ X^s_{other\ phases} \quad (4)$$

which allows to calculate the average concentration of the element in the non-silicate phases, $C^s_{other\ phases}$, and the fraction of the element inventory contained in these phases, $(1\text{-}f_{C3S} \text{-} f_{C2S})\ C^s_{other\ phases}$. These relations indicate the partition of a given element between the solid phases (C_3S, C_2S) and the melt inside the kiln. Propagation of uncertainties has to be considered, related to multiplication of modal abundance of a minor phase and concentration of trace elements; therefore, results should be considered as an approximation.

Tables V and VI present the distribution of selected element (P, S, Sr, Mg), considering the total among of the respective oxides in each sample and the fraction (%) of this amount which is contained in C_3S, C_2S and other phases (interstitial), based in the calculations discussed above. As distribution is based on modal composition of the samples, results are presented considering modal composition determined both by point counting under the electron microscope (Table V) and by XRD-Rietveld (Table VI); both Tables display the same trends, with minor variations.

Average concentration of P_2O_5 in C_2S (1.42 wt.%) is slightly higher than in C_3S (0.9 wt.%), however considering the higher modal abundance of C_3S, P_2O_5 in the clinker is equally distributed among C_3S and C_2S; non-silicate phases

Table V - Percentage of selected trace and minor elements among clinker phases; calculation based on modal analysis by point counting under the optical microscope.
[Tabela V - Porcentagem de elementos traços e menores selecionados distribuídos entre as fases do clínquer; cálculo baseado nos dados modais por contagem de pontos ao microscópio óptico.]

	P_2O_5	SrO	SO_3	MgO
clinker A (wt.%)	*0.82*	*0.79*	*1.24*	*6.74*
fraction in C_3S (%)	58.5	34.2	13.7	12.6
fraction in C_2S (%)	43.9	35.4	58.1	1.0
fraction in other phases (%)	-2.4	30.4	28.2	86.4
clinker B (wt.%)	*0.88*	*0.77*	*1.93*	*6.73*
fraction in C_3S (%)	48.8	28.6	9.8	7.6
fraction in C_2S (%)	64.8	54.5	40.4	3.3
fraction in other phases (%)	-13.6	16.8	49.7	89.1
clinker C (wt.%)	*0.88*	*0.79*	*1.77*	*6.71*
fraction in C_3S (%)	50.0	34.2	9.0	10.7
fraction in C_2S (%)	45.5	41.8	32.8	1.1
fraction in other phases (%)	4.5	24.0	58.2	88.2

Table VI - Percentage of selected trace and minor elements among clinker phases; calculation based on modal analysis by XRD-Rietveld results.
[Tabela VI - Porcentagem de elementos traços e menores selecionados distribuídos entre as fases do clínquer; cálculo baseado em dados modais obtidos por difração de raios X - método de Rietveld.]

	P_2O_5	SrO	SO_3	MgO
clinker A (wt.%)	*0.82*	*0.79*	*1.24*	*6.74*
fraction in C_3S (%)	55.6	32.9	12.9	11.9
fraction in C_2S (%)	50.0	40.5	66.0	1.0
fraction in other phases (%)	-5.6	26.6	20.1	87.1
clinker B (wt.%)	*0.88*	*0.77*	*1.93*	*6.73*
fraction in C_3S (%)	46.3	27.3	8.8	7.0
fraction in C_2S (%)	62.5	53.2	39.4	3.0
fraction in other phases (%)	-8.8	19.5	51.8	90.0
clinker C (wt.%)	*0.88*	*0.79*	*1.77*	*6.71*
fraction in C_3S (%)	49.4	34.2	9.0	10.7
fraction in C_2S (%)	46.8	44.3	33.9	1.1
fraction in other phases (%)	3.75	21.5	57.1	88.2

do not contain P_2O_5 in significant amounts. Negative values obtained in mass balance calculation reflect error propagation of data of different types (XRF, electron microprobe, XRD/optical microscopy). Phosphorous is entirely contained in Ca-silicates and, therefore, has no affinity with the melt inside the kiln.

Average SrO content in C_2S (1.11 wt.%) is twice as high as in C_3S (ca. 0.5 wt.%). The main reservoir of strontium in the clinker is C_2S which contains half of the total amount, followed by the interstitial phases and by C_3S.

Average SO_3 content in C_2S (2.29 wt.%) is seven times higher compared to C_3S (0.3 wt.%), while the main reservoir of sulfur are the alkaline sulfates, whose abundance is mainly limited by the of K_2O contents (0.27 wt. %) in the present clinker samples. A fraction of sulfur is lost by volatilization. [21] already observed that sulfur is preferentially contained in C_2S, which is stabilized and inhibiting its reaction with CaO. Similar conclusions are presented by [22], who also reported that sulfur concentration in C_2S is typically between four and five times that in C_3S, which is approximately the same as the ratio of C_3S to C_2S in many present-day clinkers.

The distribution of MgO is strongly controlled by the crystallization of cubic MgO in the interstitial phases. Among the Ca-silicates, Mg has a stronger preference to C_3S (MgO = 1.38 wt.%) compared to C_2S (MgO = 0.36 wt.%). The present study confirms this situation, with MgO mainly concentrated in other phases (periclase), followed by C_3S and, in lesser amount, by C_2S.

Zinc contents are low in both C_3S (0.04 to 0.02 wt.%) and C_2S (0.02 wt.%). The absolute amount of Zn is fairly low in the clinker (between 70 and 570 ppm), and is close to the detection limit of the electron microprobe in the Ca-silicate analysis, which produces analytical biases in mass balance calculations.

CONCLUSIONS

The comparison of industrial clinkers produced with different fuel compositions indicated that TDF does not significantly alter clinker microtexture and mineral composition. The more reliable indicator of TDF use is Zn content, which is around seven times higher in clinkers produced with TDF, compared with clinkers produced in the same kiln and with the same raw-materials, but without TDF. Fuel composition do not significantly affect the composition of Ca-silicates, which composition is more closely related to the raw-materials composition.

Phosphorous is derived from the raw-materials, particularly in apatite-rich rocks such as carbonatites and phosorites, but can also be introduced in the kiln via cofiring of animal carcasses. Phosphorous substitutes silicon in tetrahedral sites, in similar proportions in both C_3S and C_2S; given its modal abundance, C_3S is the main phosphorous reservoir in the clinker.

Sulfur is present in the studied system due to the presence of petroleum coke in the fuel mix. It is preferentially partitioned toward C_2S compared to C_3S, in substitution for Si^{4+} in tetrahedral sites. Sulfur also forms alkaline sulphates, which are limited by the availability of K^+ and Na^+, and is in part lost due to its high volatility.

Strontium is a rare element in the Earth's crust, but occurs in relatively high contents in carbonatites (10.000 ppm in average). In Portland clinker, Sr^{2+} substitutes for Ca^{2+}, mainly in C_2S and in non-silicatic phases.

Magnesium is mainly concentrated in interstitial phases (periclase), followed by C_3S and, in lesser amount, by C_2S.

ACKNOWLEDGEMENTS

REFERENCES

[1] K. Bell, *Carbonatites: Genesis and evolution*, 1st Edition, Springer Verlag, Berlin, Germany (1989) 618 p.

[2] Ministry for Mines and Energy, Brazilian Energy Balance - year 2012, Brasília (Brasil) (2013) available at https://ben.epe.gov.br/downloads/Relatorio_Final_BEN_2013.pdf, accessed in 14/09/2013

[3] C. B. Gomes, E. Ruberti, L. Morbidelli, J. S. Am. Earth Sci. **3** (1990) 51.

[4] R. D. Shannon, Acta Crystallographica A**32** (1976) 751.

[5] W. G. Mumme, Neues Jahrbuch fuer Mineralogie **4** (1995) 145.

[6] W. G. Mumme, R. J. Hill, G. W. Bushnell, E. R. Segnit, Neues Jahrbuch fuer Mineralogie Abhandlungen **169** (1995) 35.

[7] P. Mondal, J. W. Jeffery, Acta Crystallographica B **31** (1975) 689.

[8] A. A. Colville, S. Geller, Acta Crystallographica B **27** (1971) 2311.

[9] S. Sasaki, K. Fujino, Y. Takeuchi, Proceedings of the Japan Academy **55** (1979) 43.

[10] G. Natta, L. Passerini, Gazzetta Chimica Italiana **59** (1929) 129.

[11] L. Desgranges, D. Grebille, G. Calvarin, G. Chevrier, N. Floquet, J. C. Niepce, Acta Crystallographica B**49** (1993) 812.

[12] J. I. Bhatty, "Research and Development Bulletin RD109T", Portland Cement Association, Skokie, IL, USA (1995).

[13] R. W. Nurse, J. Appl. Chem. **2** (1952) 708.

[14] K. Akatsu, K. Maeda, I. Ikeda, "The effect of Cr_2O_3 and P_2O_5 on the strength and colour of portland cement clinker", C.A.J., Review of the 24th General Meeting **24** (1970) 20-23.

[15] L. Halicz, Y. Nathan, L. Bem-Dor, Cem. Concr. Res. **14** (1983) 11.

[16] L. B. McCusker, R. B. Von Dreele, D. E. Cox, D. Louer, P. Scardi. J. Appl. Crystallography **32** (1999) 36.

[17] B. H. Toby, Powder Diffraction **21**, 1 (2006) 67.
[18] D. Stephan, R. Mallmann, D. Knofel, R. Hardtl, Cem. Concr. Res. **29** (1999) 1949.
[19] D. Stephan, H. Maleki, D. Knofel, B. Iber, R. Hardtl, Cem. Concr. Res. **29** (1999) 651.

[20] H. F. W. Taylor, *Cement chemistry*, 2nd. Edition, London, England, Thomas Telford Publishing (1997) 480 p.
[21] K. G. Kolovos, S. Tsivilis, G. Kakali, J. Thermal Analysis Calorimetry **77** (2004) 759.
[22] H. F. W. Taylor, Cem. Concr. Res. **29** (1999) 1173.